Journal of Gastrointestinal Surgery (2019) 23:2372–2382
https://doi.org/10.1007/s11605-019-04140-0

ORIGINAL ARTICLE

Nomogram to Assist in Surgical Plan for Hepatocellular Carcinoma: a Prediction Model for Microvascular Invasion

Shengtao Lin[1] · Feng Ye[2] · Weiqi Rong[1] · Ying Song[2] · Fan Wu[1] · Yunhe Liu[1] · Yiling Zheng[1] · Tana Siqin[1] · Kai Zhang[1] · Liming Wang[1] · Jianxiong Wu[1]

Received: 25 November 2018 / Accepted: 23 January 2019 / Published online: 28 February 2019

Abstract

Background Microvascular invasion (MVI) relates to poor survival in hepatocellular carcinoma (HCC) patients. In this study, we aim at developing a nomogram for MVI prediction and potential assistance in surgical planning.

Methods A total of 357 patients were assigned to training ($n = 257$) and validation ($n = 100$) cohort. Univariate and multivariate analyses were used to reveal preoperative predictors for MVI. A nomogram incorporating independent predictors was constructed and validated. Disease-free survival was compared between patients, and the potential of the predicted MVI in making surgical procedure was also explored.

Results Pathological examination confirmed MVI in 140 (39.2%) patients. Imaging features including larger tumor, intratumoral artery, tumor type, and higher serum AFP independently correlated with MVI. The nomogram showed desirable performance with an AUROC of 0.803 (95% CI, 0.746–0.860) and 0.814 (95% CI, 0.720–0.908) in the training and validation cohorts, respectively. Good calibration were also revealed by calibration curve in both cohorts. The decision curve analysis indicated that the prediction nomogram was of promising usefulness in clinical work. In addition, survival analysis revealed that patients with positive-predicted MVI suffered a higher risk of early recurrence ($P < 0.01$). There was no difference in disease-free survival between anatomic or non-anatomic resection in large HCC or small HCC without nomogram-predicted MVI. However, anatomic resection improved disease-free survival in small HCC with nomogram-predicted MVI.

Conclusions The nomogram obtained desirable results in predicting MVI. Patients with predicted MVI were associated with early recurrence and anatomic resection was recommended for small HCC patients with predicted MVI.

Keywords Hepatocellular carcinoma · Microvascular invasion · Imaging features · Nomogram · Anatomic resection

Introduction

Hepatocellular carcinoma (HCC) ranks as the third leading cause of cancer death.[1] Although HCC can potentially be cured through liver transplantation or resection at early stage, the long-term survival outcomes are still far from satisfactory due to recurrence rates up to 70% within 5 years.[2] The invasion of tumor cells in the intrahepatic vessels is defined as microvascular invasion (MVI) and relates to the aggressiveness of HCC. Together with tumor size, number, differentiation, and some other factors, MVI is well-acknowledged as predictor for unfavorable prognosis.[3,4] However, the diagnosis of MVI can only be acquired through pathological examination after surgery, which has little value in preoperative management.

Many efforts have been taken to illustrate the relationships between MVI and preoperative parameters. Serum alpha-

Electronic supplementary material The online version of this article (https://doi.org/10.1007/s11605-019-04140-0) contains supplementary material, which is available to authorized users.

✉ Liming Wang
stewen_wang@sina.com

✉ Jianxiong Wu
dr_wujx@126.com

[1] Department of Hepatobiliary Surgery, National Cancer Center/ National Clinical Research Center for Cancer/Cancer Hospital, Chinese Academy of Medical Sciences and Peking Union Medical College, No. 17 Panjiayuan NanLi, Chaoyang District, Beijing, China

[2] Department of Diagnostic Radiology, National Cancer Center/ National Clinical Research Center for Cancer/Cancer Hospital, Chinese Academy of Medical Sciences and Peking Union Medical College, Beijing, China

fetoprotein (AFP)[5,6] and des-gamma-carboxy prothrombin (DCP)[7,8] have been proved to be predictors for MVI in patients with HCC. However, the cutoff values of serum biomarkers are debatable[9] and they can also abnormally elevate in patients with chronic liver diseases.[10] With the rapid development of radiological technology, magnetic resonance (MR) imaging provide reliable assessment of HCCs[11] and its potential in MVI prediction have been reported in recent years. MR imaging features such as peritumoral enhancement,[12,13] non-smooth margins,[14] and lower apparent diffusion coefficient (ADC) value[15,16] are widely used in MVI prediction. Unfortunately, which feature best reflects the presence of MVI remains controversial. In addition, it is impractical to achieve high specificity and sensibility at the same time using a single feature. There were also some attempts to construct multifactor prediction models for MVI, but the generalization ability remained ambiguity due to limited sample size,[17] and selection bias.[6] For the moment, there were still limited preoperative diagnostic models combining MR imaging features and serum biomarkers for predicting MVI. Moreover, the performance of these models in predicting patients' recurrence and making preoperative treatment decisions remained unclear.

Surgical resection is the primary treatment for HCC, but the optimal surgical strategy is under debate.[18] Ideal hepatectomy should both remove the tumor burden and preserve enough functional reserve of the diseased liver. Anatomic resection is praised for complete removal of the tumor-bearing portal territory,[19,20] but is also criticized for removal of more noncancerous, functional liver parenchyma.[21–23] Therefore, identifying individuals suitable for anatomic resection is of great importance. It was supposed that patients with unfavorable tumor characteristics, such as MVI, will benefit from anatomic resection.[24] However, there is hardly any study exploring the application of predicted MVI in making surgical procedures preoperatively.

In this study, we retrospectively analyzed clinical and imaging features in patients with single HCC, aiming at revealing risk factors of MVI. We also developed and validated a preoperative diagnostic model for MVI. Moreover, we probed into its potential in making surgical procedures.

Materials and Methods

Study Population

Six hundred thirty-six consecutive HCC patients received curative liver resection at the Department of Hepatobiliary Surgery, Cancer Hospital, Chinese Academy of Medical Sciences, between January 2015 and December 2017. The inclusion criteria were listed as follows: (1) single HCC without satellite lesions, macrovascular invasion, or extrahepatic metastasis according to preoperative evaluation; (2) patients who received contrast-enhanced liver MR within 1 month before surgery, and the images were qualified for evaluation; (3) patients without previous anticancer treatment; and (4) patients without other malignancy prior to surgery. Patients with preoperatively confirmed multiple lesions or satellite nodules were excluded for the following reasons: (1) multiple tumors were categorized to more advanced stages comparing to single tumor regardless of the presence of microvascular invasion, (2) it was impossible to evaluate the effect of each tumor on elevated serum tumor markers due to the heterogeneity of HCCs, and (3) satellite nodules were probably originated from micrometastases in the intrahepatic vessels.[25]

Clinical and Pathological Characteristics

All patients received routine laboratory tests, contrast-enhanced MR, and preoperative evaluation, and then underwent curative resection. Either anatomic or non-anatomic resection was performed according to the location of the tumor, the condition of the patient's liver, and surgeon preference. All patients received contrast-enhanced computed tomography (CT) or MR every 3–6 months after surgery to evaluate intrahepatic recurrence. If necessary, chest CT scans, bone scintigraphy, or positron emission tomography-computed tomography (PET-CT) were applied to evaluate distant metastasis. Patients with elevated serum AFP were considered as suspected recurrence, and other diagnostic procedures were required. Recurrence was defined as the presence of new nodules having radiologic features compatible with HCC from two imaging modalities, or pathological confirmation of new nodules after biopsy or surgical resection. The interval between surgery and the diagnosis of the first recurrence was defined as disease-free survival (DFS). The last follow-up date was November 10, 2018.

The pathological criteria for HCC were detailed in the previous study.[26] Briefly speaking, the specimen were cut consecutively at the maximal diameter and fixed within 30 min after surgical removal, followed by seven-point baseline sampling. Both sampling from adjacent peritumoral liver tissues (≤ 1 cm from tumor margin) and distant peritumoral liver tissues (> 1 cm from tumor margin) were conducted to evaluate MVI. Cancer cell nest in the endothelial vascular lumen was defined as MVI, including intra-tumoral and extra-tumoral MVI. CD34 staining was conducted to assist MVI identification if necessary.

MR Imaging Protocol

All MR imaging was performed using a 3.0-T MR system (Discovery MR750 3.0 T, GE, USA) with an eight-element phased-array wrap-around surface coil. The baseline MR imaging included the following sequences: (1) T1-weighted, in-phase and opposed-phase sequence (TR 300 ms, TE 2.4/

5.8 ms, flip angle 80°, matrix size 288*192, NEX 0.75, section thickness 5–8 mm, field of view (FOV) 35–42 cm, breath hold 18–21 s); (2) T2-weighted sequence (TR 6000–8000 ms, TE 90 ms, ETL 14–21, matrix size 288*224, NEX 2, section thickness 5–8 mm, FOV 35–42 cm); and (3) diffusion-weighted images (DWI) were acquired using respiratory-triggered, single-shot, echo-planar imaging (TR: 6000–8000 ms, TE 65.8 ms, matrix size 128*128, NEX 2, section thickness 5–8 mm, FOV 35–42 cm) with *b* values of 800 s/mm^2.

Dynamic imaging was acquired using liver acquisition with volume acceleration-extended volume (LAVA-XV) sequence (TR/TE 3.7/1.1 ms, flip angle 15°, matrix size 288*192, section thickness 4–4.8 mm, FOV 35–42 cm). Arterial, portal venous, and equilibrium phase images were obtained at 20–25 s, 65 s, and 2 min after the injection of gadolinium-based contrast media, respectively.

Image Analysis

Two specialist radiologists (F.Y. and Y.S. with 15 and 13 years' experience in MR diagnosis, respectively) who were blind to the patients' clinical, pathological, and follow-up information reviewed the preoperative MR images. After independently evaluation, a discussion was required to reach a consensus when a discrepancy occurred.

Intra-tumoral hemorrhage was defined as hyperintense portion inside the tumor both in the fat-saturated T1-weighted sequence and opposed-phase images (Fig. 1(A)). The presence of intra-tumoral fat[27] was defined as an area of tumor with a signal intensity decrease in opposed-phase compared with the in-phase image (Fig. 1(B)). Intra-tumoral artery is the presence of discontinuous and tortuous arterial enhancement within the tumor in arterial phase (Fig. 1(C)).[28] Intra-tumoral necrosis referred to a region within the tumor that showed an absence of enhancement on multiphasic contrast-enhanced MR (Fig. 1(D)).

Single nodule with a smooth margin was categorized according to the existence of radiologic capsule. The capsule was assessed in the portal venous or equilibrium phases and related to a thin liner-enhancing structure enveloping the tumor. Radiological capsule enveloping more or less than 90% of the tumor referred to a complete or incomplete capsule, respectively. A situation where no radiological capsule could be identified was defined as an absence of capsule (Fig. 1(E)). With reference to previous study,[29] nodules with nonsmooth margin were divided into three types as follows. Focal extranodular extension related to a tumor with a minute budding portion at its periphery protruding into the liver parenchyma (Fig. 1(F)). A tumor had an irregular surface and unclear boundaries with liver parenchyma were defined as focal infiltrative margin (Fig. 1(G)). Multinodular confluent appearance referred to those irregular lesions formed by a cluster of small, contiguous nodules, and irregular linear enhancement inside the lesions could be observed in the portal venous phase (Fig. 1(H)).

The tumor diameter was measured in both axial and coronal images and the maximum was recorded. The signal intensity (SI) was measured by drawing regions of interest (ROIs) in the tumor and hepatic parenchyma on DWI with *b* value of 800 s/mm^2. The area of necrosis, hemorrhage, and main vessels were excluded during the measuring process. The ratio between SI of the tumor and normal hepatic parenchyma was recorded as DWI ratio. Similar processes were performed in measuring the ADC values on the ADC map, with reference to the DWI. Mean value of each tumor was calculated after triple measurement.[30]

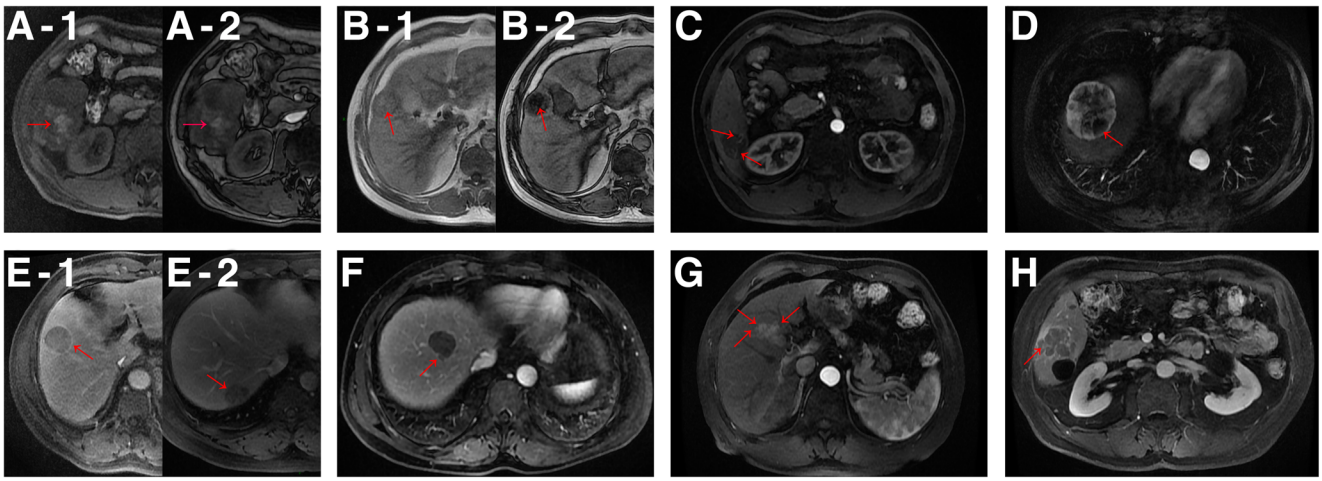

Fig. 1 Illustrations of imaging features on contrast-enhanced magnetic resonance imaging. (A) Tumor with intra-tumoral hemorrhage in the fat-saturated T1-weighted sequence (A-1) and the opposed-phase T1-weighted image (A-2). (B) Tumor with intra-tumoral fat in the in-phase T1-weighted image (B-1) and the opposed-phase T1-weighted image (B-2). (C) Tumor with intra-tumoral artery in the arterial phase. (D) Tumor with intra-tumoral necrosis in the arterial phase. (E) Single tumor with a smooth margin was enveloped by a capsule (E-1) or was not enveloped by a capsule (E-2). (F) Tumor with a minute budding portion protruding into the peritumoral parenchyma. (G) Tumor with focal infiltrative margin. (H) Tumor with multinodular confluent appearance

Statistical Analysis

Continuous variables were displayed as mean and standard deviation, and categorical variables were presented as number and percentages. In addition, serum AFP was skewed distributed and adjusted using log transformation (Log 10). Two-sample *t* test or the Wilcoxon signed-rank test was performed to analyze continuous variables. Chi-square or Fisher's exact test was used to analyze categorical variables. Interobserver agreement for image features was analyzed using the Cohen kappa coefficient.

The relationship between preoperative characteristics and MVI was analyzed using univariate logistic regression analysis, and parameters with statistical significance entered into the multivariate logistic regression analysis. A nomogram was constructed using these independent predictors. The cut-off value of the nomogram was determined according to receiver operating characteristic (ROC) curve. The area under the receiver operating characteristic curve (AUROC), the Hosmer-Lemeshow chi-square test, and calibration plots were conducted to assess model discrimination and calibration. Decision curve analysis (DCA) was applied to probe into the clinical usefulness. The difference of DFS between two groups was analyzed using the Kaplan-Meier curves. Statistical analyses were conducted using R, version 3.5. Nomogram was developed using *rms* package. A *P* value less than 0.05 was considered as statistical significance.

Results

Clinical and Imaging Characteristics

A total of 636 HCC patients received liver resection during the study period, and 357 qualified patients were enrolled in the final study (Figure S1). This group included 54 females and 303 males with a mean age of 56 ± 10.20 (range, 25–86) years. Histological examination confirmed MVI in 140 (39.2%) of these patients. The numbers of patients infected by hepatitis B, hepatitis C, and combined hepatitis B and C virus were 251, 19, and 7, respectively. The remaining 80 patients were free from hepatitis virus infection. The patients who received surgery between January 2016 and December 2017 were assigned into the training cohort ($n = 257$), and remaining patients were assigned into the validation cohort ($n = 100$).

The clinical and imaging characteristics of the patients are summarized in Table 1. Baseline characteristics were similar in the two cohorts. The interobserver agreement between imaging features is listed in Table S1, and the agreement between different observers was more than 0.75 for all features.

Preoperative Predictor for Presence of MVI Based on Univariate and Multivariate Analysis

The results of the univariate analysis of the clinical and imaging features in the training cohort are listed in Table 2. Serum AFP, intra-tumoral artery, and tumor diameter were significantly associated with MVI in HCC patients ($P < 0.001$). Tumor type and tumor capsule also related to the presence of MVI ($P < 0.05$). Among five different categories in tumor type, a tumor with extranodular extension, infiltrative margin, and multinodular confluence suffered higher risk of the presence of MVI than a tumor with smooth margin and capsule (OR = 2.62, $P = 0.011$; OR = 2.57, $P = 0.012$; OR = 11.5, $P < 0.001$; respectively). Comparing to a complete capsule, a tumor with an incomplete capsule is more prone to MVI (OR = 2.33, $P = 0.009$).

All the significant predictors were included in the multivariate analysis. On multivariate analysis, serum AFP ($P = 0.009$), intra-tumoral artery ($P < 0.001$), tumor type ($P = 0.034$), and tumor diameter ($P = 0.044$) were independently associated with presence of MVI (Table 2).

Development and Validation of a Nomogram for Preoperative MVI Prediction

A nomogram incorporating the four predictors was developed using the results from the multivariate analysis (Fig. 2). The probability of MVI could be estimated with the help of the nomogram. The cutoff value was set at 140 according to the ROC curve in the training cohort. The sensitivity and specificity were 83.0% and 68.9% in the training cohort and 82.4% and 59.1% in the validation cohort, respectively. The performance of the model was desirable in predicting MVI, with an AUROC of 0.803 (95% CI, 0.746–0.860) in the training cohort (Fig. 3a) and 0.814 (95% CI, 0.720–0.908) in the validation cohort (Fig. 3b), respectively. Calibration curves and the Hosmer-Lemeshow test demonstrated acceptable model calibration, with good agreement between the predicted MVI and histopathologic confirmation in both training cohort and validation cohort (chi-square: 4.96, $P = 0.84$, chi-square: 5.51, $P = 0.79$, respectively; Fig. 3c, d). DCA for the nomogram is presented in Fig. 3e, f. The DCA revealed that using the nomogram to predict MVI will probably add more benefit than treating either all or no patients in both cohorts.

Survival Analysis of Patients with Single HCC After Curative Resection

Two patients that died within 90 days after surgery and one patient who received salvage liver transplantation due to hepatic failure after surgery were excluded. Among the remaining patients, 34 patients received TACE (transhepatic arterial chemotherapy and embolization), and 19 patients received

Table 1 Clinical and radiologic characteristics in the training and the validation cohort

Characteristic	Training cohort Jan 2016~Dec 2017 ($n = 257$), no. (%)	Validation cohort Jan 2015~Dec 2015 ($n = 100$), no. (%)	*P* value
Age (years)			0.250
≤ 60	166 (64.6)	71 (71.0)	
> 60	91 (35.4)	29 (29.0)	
Sex			0.967
Female	39 (15.2)	15 (15.0)	
Male	218 (84.8)	85 (85.0)	
Hepatitis virus infection			0.554[a]
None	54 (21.0)	26 (26.0)	
HBV	186 (72.4)	65 (65.0)	
HCV	12 (4.7)	7 (7.0)	
HBV + HCV	5 (1.9)	2 (2.0)	
Diabetes			0.096
Absence	53 (20.6)	13 (13.0)	
Presence	204 (79.4)	87 (87.0)	
MVI			0.208
Absence	151 (58.8)	66 (66.0)	
Presence	106 (41.2)	34 (34.0)	
logAFP, ng/ml	1.54 ± 1.12	1.72 ± 1.18	0.219
Imaging features			
Intra-tumoral hemorrhage			0.227
Absence	228 (88.7)	93 (93.0)	
Presence	29 (11.3)	7 (7.0)	
Intra-tumoral fat			0.224[a]
Absence	205 (79.8)	86 (86.0)	
Presence	52 (20.2)	14 (14.0)	
Intra-tumoral artery			0.262
Absence	180 (70.0)	76 (76.0)	
Presence	77 (30.0)	24 (24.0)	
Intra-tumoral necrosis			0.105[a]
Absence	163 (63.4)	73 (73.0)	
Presence	94 (36.6)	27 (27.0)	
Tumor type			0.359
Smooth margin with capsule	68 (26.5)	26 (26.0)	
Smooth margin without capsule	35 (13.6)	21 (21.0)	
Focal extranodular extension	60 (23.3)	16 (16.0)	
Focal infiltrative margin	65 (25.3)	25 (25.0)	
Multinodular confluence	29 (11.3)	12 (12.0)	
Capsule			0.714
Complete	114 (44.4)	45 (45.0)	
Incomplete	61 (23.7)	27 (27.0)	
Absence	82 (31.9)	28 (28.0)	
Diameter, cm	3.98 ± 1.98	3.86 ± 1.82	0.8393
ADC value, $\times 10^{-3}$ mm^2/s	1.21 ± 0.29	1.27 ± 0.32	0.104
Tumor-to-liver SI ratio on DWI	3.48 ± 2.14	3.17 ± 1.53	0.356

HBV hepatitis B virus, *HCV* hepatitis C virus, *AFP* alpha-fetoprotein, *ADC* apparent diffusion coefficient, *SI* signal intensity, *DWI* diffusion-weighted imaging

[a] Fisher's exact test was performed

Table 2 Preoperative predictors for MVI in patients with single HCC in the training cohort

Characteristic	Univariate analysis		Multivariate analysis	
	OR (95% CI)	*P* value	OR (95% CI)	*P* value
Age, > 60 vs ≤ 60, years	1.03 (0.61, 1.74)	0.902	–	
Sex, male vs female	1.01 (0.51, 2.02)	0.976	–	
Etiology				
HBV vs none	0.93 (0.5, 1.72)	0.82	–	
HCV vs none	1.35 (0.38, 4.72)	0.641	–	
HBV + HCV vs none	0.34 (0.04, 3.22)	0.345	–	
Diabetes	0.75 (0.4, 1.41)	0.371	–	
logAFP, ng/ml	1.7 (1.34, 2.15)	< 0.001*	1.44 (1.09, 1.9)	0.009*
Imaging features				
Intra-tumoral hemorrhage	1.38 (0.64, 2.99)	0.416	–	
Intra-tumoral fat	0.96 (0.51, 1.78)	0.888	–	
Intra-tumoral artery	6.32 (3.5, 11.42)	< 0.001*	3.57 (1.72, 7.42)	< 0.001*
Intra-tumoral necrosis	1.54 (0.92, 2.57)	0.102	–	
Tumor type		< 0.001*		0.034*
Smooth margin with capsule	Reference		Reference	
Smooth margin without capsule	0.89 (0.34, 2.32)	0.81	1.89 (0.4, 8.91)	0.422
Focal extranodular extension	2.62 (1.24, 5.54)	0.011	2.34 (1, 5.5)	0.051
Focal infiltrative margin	2.57 (1.23, 5.36)	0.012	3.02 (0.84, 10.85)	0.091
Multinodular confluence	11.5 (4.01, 32.96)	< 0.001	8.03 (1.73, 37.36)	0.008
Capsule		0.028*		0.866
Incomplete vs complete	2.33 (1.23, 4.4)	0.009	1.13 (0.34, 3.72)	0.844
Absence vs complete	1.18 (0.66, 2.13)	0.573	0.89 (0.24, 3.24)	0.856
Diameter	1.5 (1.29, 1.74)	< 0.001*	1.21 (1.01, 1.46)	0.044*
ADC value, $\times 10^{-3}$ mm^2/s	0.36 (0.14, 0.93)	0.036*	0.5 (0.16, 1.52)	0.22
Tumor-to-liver SI ratio on DWI	1.09 (0.97, 1.23)	0.145	–	

HBV hepatitis B virus, *HCV* hepatitis C virus, *AFP* alpha-fetoprotein, *ADC* apparent diffusion coefficient, *SI* signal intensity, *DWI* diffusion-weighted imaging

*Significant difference

IMRT (intensity modulated radiation therapy) after curative resection in order to reduce recurrence risk. Patients with either pathologically confirmed or nomogram-predicted MVI suffered higher risk of early recurrence (Figure S2, $P < 0.01$, and $P < 0.01$, respectively). The differences between patients' disease-free survival according to surgical procedures are displayed in Figure S3. No significant difference was observed between patients who received anatomic resection and non-anatomic resection in the entire cohort or patients with large tumor (> 5 cm) (Figure S3A, $P = 0.26$ and Figure S3B, $P = 0.97$ respectively). But a borderline significant trend (Figure S3C, $P = 0.09$) was detected between

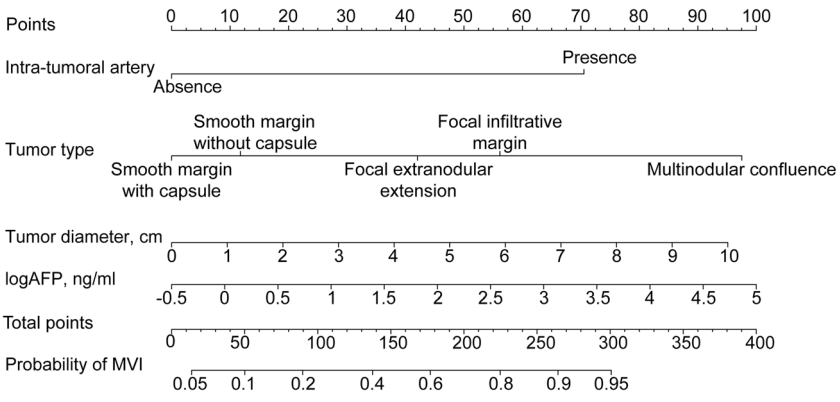

Fig. 2 Nomogram predicting the probability of MVI in HCC patients. Total points were calculated by adding up the points of each variable on the point scale and indicated the probability of MVI presence according to the bottom scales. AFP alpha-fetoprotein

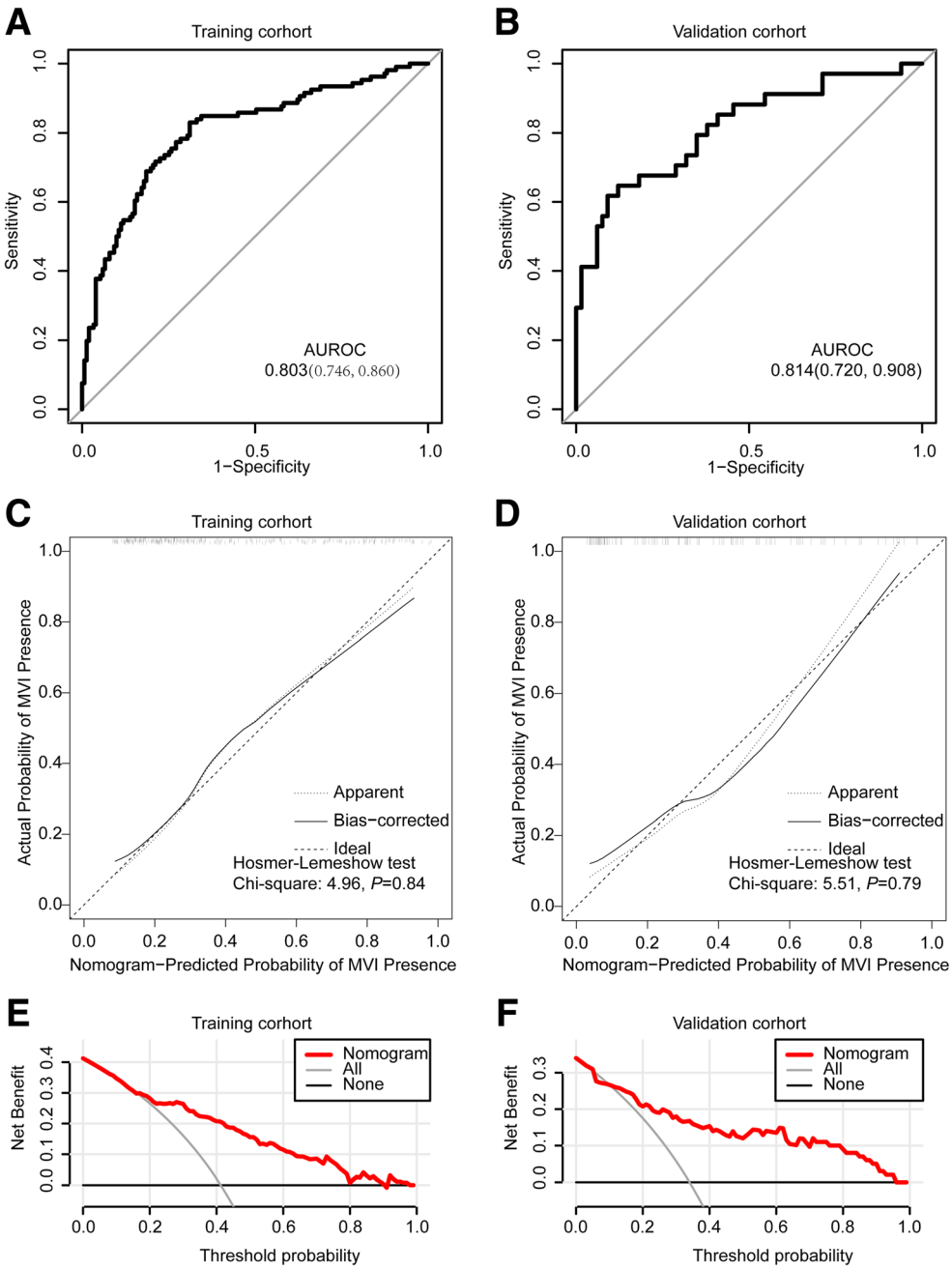

Fig. 3 Validation of the preoperative MVI prediction nomogram. The ROC curves of the nomogram in the training cohort (**a**, AUROC: 0.803) and the validation cohort (**b**, AUROC: 0.814), respectively. The area under the ROC (AUROC) represents the probability that a randomly chosen individual is correctly diagnosed with greater suspicion than a randomly chosen negative individual. The calibration curves for predicting MVI presence in the training cohort (**c**) and the validation cohort (**d**), respectively. Nomogram-predicted MVI presence is plotted on the *X*-axis, and the actual MVI presence is plotted on the *Y*-axis. A plot along the 45° line would indicate a perfect calibration model in which the predicted presence are identical to the actual presence. The distribution of the predicted probabilities of MVI presence is shown at the top of the graphs. Decision curve analysis (DCA) for the nomogram in the training cohort (**e**) and the validation cohort (**f**), respectively. The gray or black line hypothesizes that all patients were MVI positive or negative, respectively. The red line represents the net benefit of the nomogram at different threshold probabilities

different surgical procedures in patients with small tumor (≤ 5 cm). Then, we probed into the impact of surgical procedures on patients' disease-free survival in patients with small HCC (≤ 5 cm). There was no difference between different surgical procedures in patients without presence of pathological confirmed MVI or nomogram-predicted MVI (Fig. 4a, $P = 0.50$, and Fig. 4b, $P = 0.54$, respectively). However, anatomic resection seemingly improved the disease-free survival of small HCC patients with either histopathological confirmed MVI or nomogram-predicted MVI (Fig. 4c, $P = 0.08$, and Fig. 4d, $P = 0.06$, respectively). Furthermore, significant differences were observed between different surgical procedures in patients with small HCCs (MVI-positive or pred.MVI-positive) who did not receive postsurgical adjuvant treatment (Fig. 4e, $P = 0.03$ for histopathological confirmed MVI, and Fig. 4f, $P = 0.04$ for nomogram-predicted MVI, respectively).

Discussions

Microvascular invasion has been accepted worldwide as an unfavorable predictor for HCC patients. In the present study, we demonstrated that preoperative features including serum AFP, intratumoral artery, tumor type, and tumor diameter are independently

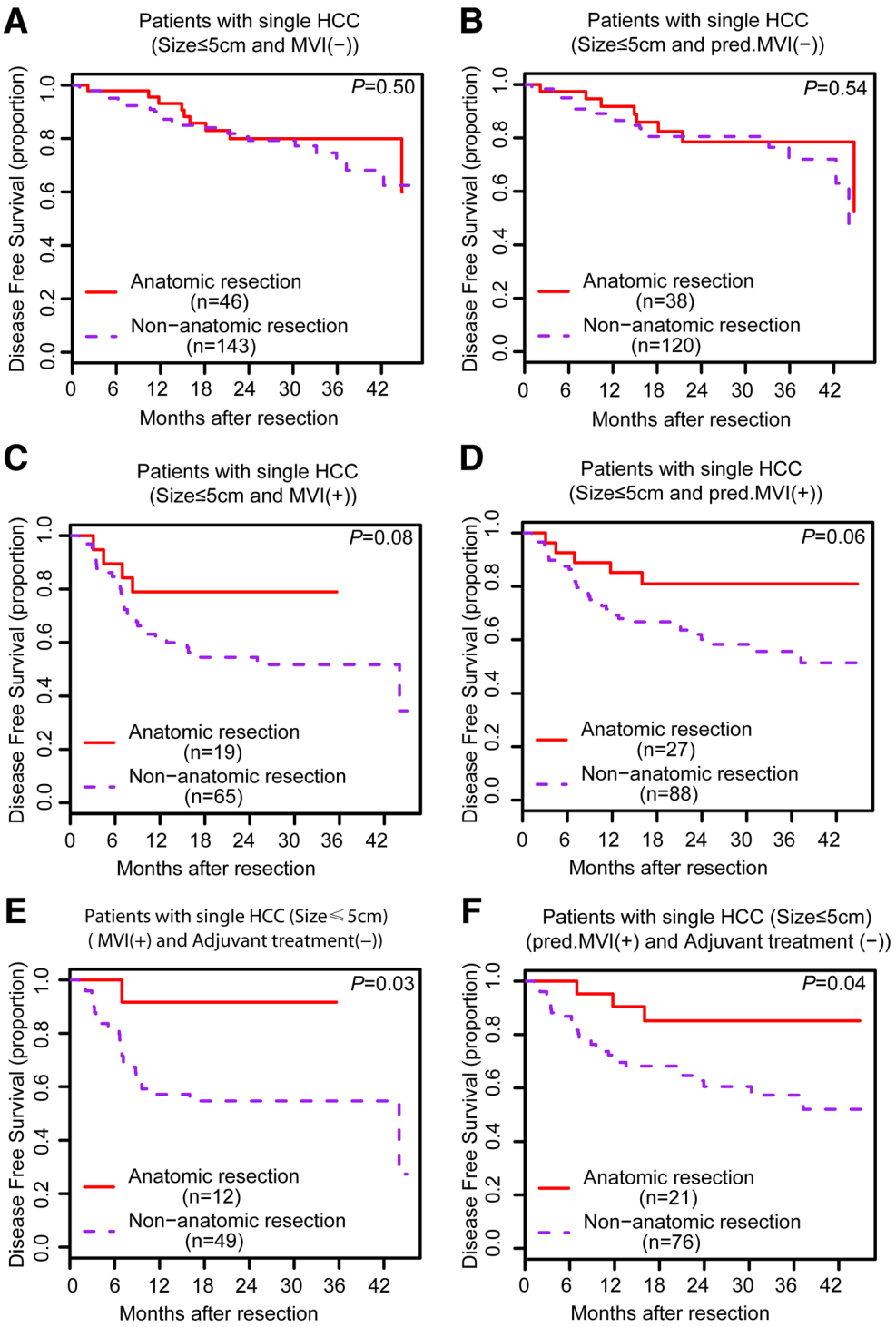

Fig. 4 Disease-free survival between small HCC patients received different surgical procedures. The Kaplan-Meier survival curves and the log-rank test compared the disease-free survival in the small HCC patients without MVI (**a**, $P = 0.50$) or pred.MVI (**b**, $P = 0.54$), the small HCC patients with MVI (**c**, $P = 0.08$) or pred.MVI (**d**, $P = 0.06$), the small HCC patients with MVI and without adjuvant therapy (**e**, $P = 0.03$), the small HCC patients with pred.MVI and without adjuvant therapy (**f**, $P = 0.04$). MVI microvascular invasion, pred-MVI the nomogram-predicted MVI)

associated with the presence of MVI. Furthermore, we developed and validated a nomogram for preoperative MVI prediction incorporating these features for patients with single HCC. The nomogram is also useful in identifying patients with high risk of recurrence before surgery. Anatomic resection showed an evident correlation with decreased tumor recurrence rate in small HCC patients with nomogram-predicted MVI, who did not receive adjuvant therapy.

Previous findings demonstrated that larger tumor and higher serum AFP related to more aggressive behaviors[5,31] and our study further proved their positive relationship with the possibility of MVI in early-stage HCCs. We also found that intra-tumoral arteries were more frequent in patients with MVI. Previous studies reported that intra-tumoral vessels related to the poorer differentiation,[32] angiogenesis, cellular proliferation, and matrix invasion.[33] These results could explain

the invasiveness of tumor with intra-tumoral arteries at pathological level and biological behavior. Furthermore, nonsmooth margin was a significant predictor for MVI in our study, and the results were similar to previous researches.[29] Confluent multinodular tumors were reported to be related to high incidence of different DNA ploidy patterns or DNA indices,[34] which may reflect the genetic alteration in the occurrence and development of HCC. It was also suggested that numerous vessels could be engulfed in the tumor when several small nodules fused together generating tumor with multinodular confluence, resulting in a high frequency of microvascular invasion.[35] The remaining two types of nonsmooth margin were predictors for MVI with a strong tendency towards statistical significance in our study. Previous articles hypothesized that extranodular extension/infiltrative margin appeared when the tumor invaded into normal liver parenchyma,[36] and MVI tended to occur at these sites.[37] A prospective study with a site by site correlation between imaging features and histopathological findings is urgently needed to confirm the hypothesis.

Furthermore, we developed a user-friendly nomogram based on noninvasive, easy-accessible parameters. In previous study, Zhao and his colleagues constructed a model for MVI prediction, but the generalization ability remained ambiguity due to the lack of validation and limited sample size (51 patients).[17] Cucchetti et al. proposed a prediction model for patients based on artificial neural network (ANN),[6] but the generalization ability of the model was questionable for the reason that the incidence of MVI in the study was 74.4%, an abnormally elevated level in HCC patients at early stage.[4] The present nomogram in our study showed desirable performance in discrimination and calibration, and was promising in clinical application. Firstly, the nomogram-predicted MVI was similar to histopathological confirmed MVI in identifying patients at high risk for recurrence preoperatively. Several respective analyses and clinical trials have illustrated that adjuvant therapy improved the outcomes of patients with MVI.[38, 39] But whether neoadjuvant treatments have similar effect remained unclear due to the unavailable diagnosis of MVI before surgery. Secondly, MVI was associated with over two-fold mortality risk in liver transplantation patients beyond Milan criteria,[40] and preoperatively predicted MVI could serve as an auxiliary criteria in patient selection. Thirdly, anatomic resection was associated with longer RFS in small HCC patients with MVI or nomogram-predicted MVI, which coincide with a previous study.[24] Anatomic resection did not bring benefit in disease-free survival in large HCC patients or small HCC patients without MVI. This phenomenon may be associated with preserving more functional reserve liver volume and relatively less aggressive biological behavior. The nomogram could provide assistance in selecting appropriate operative procedures for HCC patients. Therefore, the present preoperative MVI estimation model identified patients at high risk for recurrence and will be helpful in recruiting patients for neoadjuvant therapy, refining organ allocation system and making personalized surgical procedure.

There were still some limitations in the study. Firstly, there was no external validation using another set of patients in this study, which may impair the reliability of the nomogram. Secondly, potential selection bias was present in this study, especially in the subgroup survival analysis due to the nature of respective research and limited sample size. Thirdly, about 80% of the patients suffered from viral hepatitis infection in our study. Whether the model could be generalized to HCC patients with other liver diseases remained unknown. Further research is warranted to refine the model in the future.

Conclusion

We developed and validated a promising nomogram for preoperatively MVI estimation and may provide assistance in tailoring therapeutic choice. Patients with predicted MVI were associated with early recurrence and anatomic resection was recommended for small HCC patients with predicted MVI.

Acknowledgements We gratefully acknowledge Changfa Xia for the assistance in statistical analysis, Zhuo Li and Bo Zheng for reviewing the pathological results, and Kaijing Liu for revising the manuscript.

Authors' Contribution Study concept and design: Liming Wang, Jianxiong Wu, Weiqi Rong
Clinical data acquisition: Shengtao Lin, Yunhe Liu, Yiling Zheng
Patient follow-up: Shengtao Lin, Yunhe Liu
Imaging feature evaluation: Feng Ye, Ying Song
Statistical analysis: Shengtao Lin, Fan Wu, Feng Ye, Tana Siqi
Drafting of the manuscript: Shengtao Lin, Yiling Zheng, Liming Wang
Study supervision: Liming Wang, Jianxiong Wu
Critical revision of the manuscript: all authors

Compliance with Ethical Standards

Conflict of Interest The authors declare that they have no conflicts of interest.

References

1. Bruix J, Reig M, Sherman M. Evidence-Based Diagnosis, Staging, and Treatment of Patients With Hepatocellular Carcinoma. Gastroenterology. 2016; 150: 835–53.
2. Vitale A, Peck-Radosavljevic M, Giannini EG, Vibert E, Sieghart W, Van Poucke S, Pawlik TM. Personalized treatment of patients with very early hepatocellular carcinoma. J Hepatol. 2017; 66: 412–23.
3. Zhang X, Li J, Shen F, Lau WY. Significance of presence of microvascular invasion in specimens obtained after surgical treatment of hepatocellular carcinoma. J Gastroenterol Hepatol. 2018; 33: 347–54.

4. Rodríguez-Perálvarez M, Luong TV, Andreana L, Meyer T, Dhillon AP, Burroughs AK. A Systematic Review of Microvascular Invasion in Hepatocellular Carcinoma: Diagnostic and Prognostic Variability. Ann Surg Oncol. 2012; 20: 325–39.
5. McHugh PP, Gilbert J, Vera S, Koch A, Ranjan D, Gedaly R. Alpha-fetoprotein and tumour size are associated with microvascular invasion in explanted livers of patients undergoing transplantation with hepatocellular carcinoma. HPB (Oxford). U; 12: 56–61.
6. Cucchetti A, Piscaglia F, Grigioni AD, Ravaioli M, Cescon M, Zanello M, Grazi GL, Golfieri R, Grigioni WF, Pinna AD. Preoperative prediction of hepatocellular carcinoma tumour grade and micro-vascular invasion by means of artificial neural network: a pilot study. J Hepatol. 2010; 52: 880–8.
7. Eguchi S, Takatsuki M, Hidaka M, Soyama A, Tomonaga T, Muraoka I, Kanematsu T. Predictor for histological microvascular invasion of hepatocellular carcinoma: a lesson from 229 consecutive cases of curative liver resection. World J Surg. 2010; 34: 1034–8.
8. Pote N, Cauchy F, Albuquerque M, Voitot H, Belghiti J, Castera L, Puy H, Bedossa P, Paradis V. Performance of PIVKA-II for early hepatocellular carcinoma diagnosis and prediction of microvascular invasion. J Hepatol. 2015; 62: 848–54.
9. Gouw AS, Balabaud C, Kusano H, Todo S, Ichida T, Kojiro M. Markers for microvascular invasion in hepatocellular carcinoma: where do we stand? Liver Transpl. 2011; 17 Suppl 2: S72–80.
10. Sterling RK, Wright EC, Morgan TR, Seeff LB, Hoefs JC, Di Bisceglie AM, Dienstag JL, Lok AS. Frequency of elevated hepatocellular carcinoma (HCC) biomarkers in patients with advanced hepatitis C. Am J Gastroenterol. 2012; 107: 64–74.
11. Lee JM, Yoon JH, Joo I, Woo HS. Recent Advances in CT and MR Imaging for Evaluation of Hepatocellular Carcinoma. Liver Cancer. 2012; 1: 22–40.
12. Ahn SY, Lee JM, Joo I, Lee ES, Lee SJ, Cheon GJ, Han JK, Choi BI. Prediction of microvascular invasion of hepatocellular carcinoma using gadoxetic acid-enhanced MR and (18)F-FDG PET/CT. Abdom Imaging. 2015; 40: 843–51.
13. Kim H, Park MS, Choi JY, Park YN, Kim MJ, Kim KS, Choi JS, Han KH, Kim E, Kim KW. Can microvessel invasion of hepatocellular carcinoma be predicted by pre-operative MRI? Eur Radiol. 2009; 19: 1744–51.
14. Ariizumi S, Kitagawa K, Kotera Y, Takahashi Y, Katagiri S, Kuwatsuru R, Yamamoto M. A non-smooth tumor margin in the hepatobiliary phase of gadoxetic acid disodium (Gd-EOB-DTPA)-enhanced magnetic resonance imaging predicts microscopic portal vein invasion, intrahepatic metastasis, and early recurrence after hepatectomy in patients with hepatocellular carcinoma. J Hepatobiliary Pancreat Sci. 2011; 18: 575–85.
15. Xu P, Zeng M, Liu K, Shan Y, Xu C, Lin J. Microvascular invasion in small hepatocellular carcinoma: is it predictable with preoperative diffusion-weighted imaging? J Gastroenterol Hepatol. 2014; 29: 330–6.
16. Suh YJ, Kim MJ, Choi JY, Park MS, Kim KW. Preoperative prediction of the microvascular invasion of hepatocellular carcinoma with diffusion-weighted imaging. Liver Transpl. 2012; 18: 1171–8.
17. Zhao W, Liu W, Liu H, Yi X, Hou J, Pei Y, Liu H, Feng D, Liu L, Li W. Preoperative prediction of microvascular invasion of hepatocellular carcinoma with IVIM diffusion-weighted MR imaging and Gd-EOB-DTPA-enhanced MR imaging. PLoS One. 2018; 13: e0197488.
18. Akamatsu N, Cillo U, Cucchetti A, Donadon M, Pinna AD, Torzilli G, Kokudo N. Surgery and Hepatocellular Carcinoma. Liver Cancer. 2016; 6: 44–50.
19. Shindoh J, Makuuchi M, Matsuyama Y, Mise Y, Arita J, Sakamoto Y, Hasegawa K, Kokudo N. Complete removal of the tumor-bearing portal territory decreases local tumor recurrence and improves disease-specific survival of patients with hepatocellular carcinoma. J Hepatol. 2016; 64: 594–600.
20. Hasegawa K, Kokudo N, Imamura H, Matsuyama Y, Aoki T, Minagawa M, Sano K, Sugawara Y, Takayama T, Makuuchi M. Prognostic Impact of Anatomic Resection for Hepatocellular Carcinoma. Ann Surg. 2005; 242: 252–9.
21. Kang CM, Choi GH, Kim DH, Choi SB, Kim KS, Choi JS, Lee WJ. Revisiting the role of nonanatomic resection of small (< or = 4 cm) and single hepatocellular carcinoma in patients with well-preserved liver function. J Surg Res. 2010; 160: 81–9.
22. Tanaka K, Shimada H, Matsumoto C, Matsuo K, Nagano Y, Endo I, Togo S. Anatomic versus limited nonanatomic resection for solitary hepatocellular carcinoma. Surgery. 2008; 143: 607–15.
23. Hirokawa F, Kubo S, Nagano H, Nakai T, Kaibori M, Hayashi M, Takemura S, Wada H, Nakata Y, Matsui K, Ishizaki M, Uchiyama K. Do patients with small solitary hepatocellular carcinomas without macroscopically vascular invasion require anatomic resection? Propensity score analysis. Surgery. 2015; 157: 27–36.
24. Cucchetti A, Qiao GL, Cescon M, Li J, Xia Y, Ercolani G, Shen F, Pinna AD. Anatomic versus nonanatomic resection in cirrhotic patients with early hepatocellular carcinoma. Surgery. 2014; 155: 512–21.
25. Okusaka T, Okada S, Ueno H, Ikeda M, Shimada K, Yamamoto J, Kosuge T, Yamasaki S, Fukushima N, Sakamoto M. Satellite lesions in patients with small hepatocellular carcinoma with reference to clinicopathologic features. Cancer. 2002; 95: 1931–7.
26. Cong WM, Bu H, Chen J, Dong H, Zhu YY, Feng LH, Chen J, Guideline C. Practice guidelines for the pathological diagnosis of primary liver cancer: 2015 update. World J Gastroenterol. 2016; 22: 9279–87.
27. Min JH, Kim YK, Lim S, Jeong WK, Choi D, Lee WJ. Prediction of microvascular invasion of hepatocellular carcinomas with gadoxetic acid-enhanced MR imaging: Impact of intra-tumoral fat detected on chemical-shift images. Eur J Radiol. 2015; 84: 1036–43.
28. Lee S, Kim SH, Lee JE, Sinn DH, Park CK. Preoperative gadoxetic acid-enhanced MRI for predicting microvascular invasion in patients with single hepatocellular carcinoma. J Hepatol. 2017; 67: 526–34.
29. Wang WT, Yang L, Yang ZX, Hu XX, Ding Y, Yan X, Fu CX, Grimm R, Zeng MS, Rao SX. Assessment of Microvascular Invasion of Hepatocellular Carcinoma with Diffusion Kurtosis Imaging. Radiology. 2018; 286: 571–80.
30. Okamura S, Sumie S, Tonan T, Nakano M, Satani M, Shimose S, Shirono T, Iwamoto H, Aino H, Niizeki T, Tajiri N, Kuromatsu R, Okuda K, Nakashima O, Torimura T. Diffusion-weighted magnetic resonance imaging predicts malignant potential in small hepatocellular carcinoma. Dig Liver Dis. 2016; 48: 945–52.
31. Sakata J, Shirai Y, Wakai T, Kaneko K, Nagahashi M, Hatakeyama K. Preoperative predictors of vascular invasion in hepatocellular carcinoma. Eur J Surg Oncol. 2008; 34: 900–5.
32. Lee J, Lee J, Kim S, Baek J, Yun S, Kim K, Han J, Choi B. Enhancement patterns of hepatocellular carcinomas on multiphasicmultidetector row CT: comparison with pathological differentiation. Br J Radiol. 2012; 85: e573–83.
33. Segal E, Sirlin CB, Ooi C, Adler AS, Gollub J, Chen X, Chan BK, Matcuk GR, Barry CT, Chang HY, Kuo MD. Decoding global gene expression programs in liver cancer by noninvasive imaging. Nat Biotechnol. 2007; 25: 675–80.
34. Oriyama T, Yamanaka N, Fujimoto J, Ichikawa N, Okamoto E. Progression of hepatocellular carcinoma as reflected by nuclear DNA ploidy and cellular differentiation. J Hepatol. 1998; 28: 142–9.
35. Kanai T, Hirohashi S, Upton M, Noguchi M, Kishi K, Makuuchi M, Yamasaki S, Hasegawa H, Takayasu K, Moriyama N. Pathology of small hepatocellular carcinoma. A proposal for a new gross classification. Cancer. 1987; 60: 810–9.

36. Chou CT, Chen RC, Lee CW, Ko CJ, Wu HK, Chen YL. Prediction of microvascular invasion of hepatocellular carcinoma by pre-operative CT imaging. Br J Radiol. 2012; 85: 778–83.
37. Chou CT, Chen RC, Lin WC, Ko CJ, Chen CB, Chen YL. Prediction of microvascular invasion of hepatocellular carcinoma: preoperative CT and histopathologic correlation. AJR Am J Roentgenol. 2014; 203: W253–9.
38. Wang L, Wang W, Yao X, Rong W, Wu F, Chen B, Liu M, Lin S, Liu Y, Wu J. Postoperative adjuvant radiotherapy is associated with improved survival in hepatocellular carcinoma with microvascular invasion. Oncotarget. 2017; 8: 79971–81.
39. Wang Z, Ren Z, Chen Y, Hu J, Yang G, Yu L, Yang X, Huang A, Zhang X, Zhou S, Sun H, Wang Y, Ge N, Xu X, Tang Z, Lau W, Fan J, Wang J, Zhou J. Adjuvant Transarterial Chemoembolization for HBV-Related Hepatocellular Carcinoma After Resection: A Randomized Controlled Study. Clin Cancer Res. 2018; 24: 2074–81.
40. Donat M, Alonso S, Pereira F, Ferrero E, Carrion L, Acin-Gandara D, Moreno E. Impact of Histological Factors of Hepatocellular Carcinoma on the Outcome of Liver Transplantation. Transplant Proc. 2016; 48: 1968–77.